Amplitude and phase measurements of femtosecond pulse splitting in nonlinear dispersive media

Scott A. Diddams, Hilary K. Eaton, Alex A. Zozulya, and Tracy S. Clement

JILA, University of Colorado and National Institute of Standards and Technology, Boulder, Colorado 80309-0440

Received August 29, 1997

Frequency-resolved optical gating is used to characterize the propagation of intense femtosecond pulses in a nonlinear, dispersive medium. The combined effects of diffraction, normal dispersion, and cubic nonlinearity lead to pulse splitting. The role of the phase of the input pulse is studied. The results are compared with the predictions of a three-dimensional nonlinear Schrödinger equation. © 1998 Optical Society of America

OCIS codes: 320.7100, 320.7110, 190.5530.

Information about the electric field on a femtosecond time scale is a valuable tool in the study of ultrafast phenomena. This has proved to be the case in femtosecond-pulse generation, for which improvements in measurement techniques have accompanied a more comprehensive understanding of femtosecond lasers.[1–3] However, femtosecond pulse diagnostics should not be limited to the study and optimization of femtosecond sources. Knowledge of the amplitude and the phase of the electric field can be a powerful tool in the study of light–matter interactions outside the laser, as was demonstrated recently in the measurement of the nonlinear indices of various materials[4,5] and the characterization of nonlinear propagation in optical fibers.[6] Such experiments not only elucidate light–matter interactions but also test the measurement technique itself.

In this Letter we demonstrate the usefulness of frequency-resolved optical gating (FROG) for studying the nonlinear propagation of intense femtosecond laser pulses. We record the evolution of the temporal field of an intense femtosecond pulse as it splits into subpulses, and we show that the initial phase of the field plays an important role in this process. The evolution of the complex amplitude $\tilde{\mathcal{E}}(r, z, \tau)$ of a pulse in a nonlinear, dispersive medium can be described by the nonlinear Schrödinger equation

$$\frac{\partial \tilde{\mathcal{E}}}{\partial z} - \frac{i}{2k_0}\nabla_\perp{}^2\tilde{\mathcal{E}} + \frac{ik_0''}{2}\frac{\partial^2\tilde{\mathcal{E}}}{\partial \tau^2} - \frac{ik_0 n_2}{n_0}|\tilde{\mathcal{E}}|^2\tilde{\mathcal{E}} = 0, \quad (1)$$

where $k_0 = 2\pi n_0/\lambda_0$ and n_0 is the linear index of refraction at the center wavelength λ_0. The group-velocity dispersion (GVD) is determined by k_0'', which is the second derivative of k evaluated at λ_0. The local time τ is in the frame moving at the group velocity, $\nabla_\perp{}^2$ is the radial Laplacian, and n_2 is the nonlinear index of refraction. The field can be normalized such that $|\tilde{\mathcal{E}}|^2 = I$ is the intensity in watts per square centimeter. To lowest order, Eq. (1) includes the effects of diffraction, spatial self-focusing, temporal self-phase modulation, and dispersion, all of which act to give complicated spatiotemporal dynamics. During propagation in the regime of positive GVD ($k_0'' > 0$) and positive n_2, one anticipates that both dispersion and temporal self-phase modulation (SPM) will act to continuously separate the long- and short-wavelength components of the pulse, thereby lengthening the pulse. However, the inclusion of the spatial aspect of the field (diffraction and self-focusing) can result in temporal pulse splitting.[7,8] We emphasize this process in contrast to nonlinear propagation in single-mode optical fibers, where +GVD and $+n_2$ exist but pulse splitting is not observed because of the spatial constraint of the field.[9] Recent intensity autocorrelation measurements validate the predictions of pulse splitting in bulk media[10]; however, a standard intensity autocorrelation is always symmetric, hides detailed amplitude structure, and lacks phase information. The full field, as provided by the FROG measurement, gives a more comprehensive picture of the dynamics and should allow us to test the validity of Eq. (1) for describing nonlinear pulse propagation.

We use the second-harmonic form of FROG (SHG FROG)[11] to characterize the propagation of intense femtosecond pulses in fused silica. The SHG FROG measurement is a spectrally resolved noncollinear autocorrelation performed with a 100-μm piece of β-barium borate. The measurement yields a two-dimensional spectrogram from which the amplitude and the phase of the electric field can be determined with an iterative phase-retrieval algorithm.[11] All studies use the output of a 1-kHz regenerative amplifier that yields sub-100 fs pulses, spectrally centered near 800 nm. The delay stage in the correlator is scanned with a stepper motor, and exposure times are such that the signal from several hundred pulses is integrated each step. The amplified pulses are attenuated and focused with an $f = 50$-cm lens to a measured beam waist of 70 μm (FWHM of intensity) at the entrance face of the fused-silica sample (2.54-cm length). The spatial beam profile is well approximated by a Gaussian. We use an aperture after propagation through the sample to select only the on-axis portion of the beam for measurement. Because of the complexity and large bandwidth of the measured fields, we employ several checks to validate the measurements and eliminate systematic errors. The spectrum of the propagated fundamental (corrected for instrument response) is recorded and its autoconvolution is compared with the frequency

0146-9592/98/050379-03$10.00/0

marginal of the FROG measurement, thus correcting for the bandwidth limitations of the SHG FROG apparatus.[12] The same spectrum is compared with the spectrum recovered by the SHG FROG algorithm. We also make a second SHG FROG measurement, letting the initially measured field propagate through 5 cm of BK-7 glass at low intensity. The information from the second measurement is used to remove the time ambiguity of the initial measurement.

Figure 1 shows the results of successive SHG FROG measurements for increasing input powers. The intensity and the phase in the time domain are shown at the left. Independently measured spectra and the spectra recovered from the SHG FROG measurements are shown at the right. The top row [Fig. 1(a)] is the measured input field, with an intensity FWHM of 92 fs. The time–bandwidth product is 0.6, and some uncompensated second- and third-order phase variations are evident. Moving down the rows of Fig. 1, we see the pulse undergo an initial splitting and then multiple splittings. The fully split pulses of Figs. 1(c) and 1(d) have FWHM durations of the order of 50 fs, nearly 2× shorter than the input. With the instanteous frequency defined as $\omega_{\text{inst}} = \omega_0 - \mathrm{d}\phi/\mathrm{d}t$, the predominant negative curvature of the temporal phase implies upchirped pulses. The calculated critical power for self-focusing is $P_{\text{crit}} = (0.61\lambda_0)^2\pi/(8n_0n_2) = 2.6$ MW, where $n_0 = 1.45$, $n_2 = 2.5 \times 10^{16}$ cm^2/W, and $\lambda_0 = 800$ nm.[13] The measured peak powers for Figs. 1(b), Fig. 1(c), and Fig. 1(d) are then given by $1.7P_{\text{crit}}$, $1.9P_{\text{crit}}$, and $2.3P_{\text{crit}}$, respectively. The associated spectra of the right-hand column of Fig. 1 show pronounced broadening and modulation, with the characteristic modulation frequency being equal to the inverse of the time spacing between the pulses. Agreement between the measured and the recovered spectra is considered good in view of the complicated structure. The spectra of Figs. 1(c) and 1(d) have wings characteristic of weak continuum generation, and at the highest power weak orange-red light was visible by eye. The advantage that the SHG FROG measurement brings to this study is further illustrated by Fig. 2, where we present the measured intensity autocorrelation for the field given in Fig. 1(d). As seen, the intricate amplitude features of Fig. 1(d) are lost in the correlation.

From a simple physical standpoint, we understand the process of pulse splitting as follows: Initially, strong self-focusing moves off-axis energy toward the peak of the pulse and compresses it in both space and time.[14] As the peak intensity increases, the process of SPM also increases, thereby generating new frequency components. The combination of the SPM-induced upchirp and +GVD then act to push the energy away from $\tau = 0$, initiating the pulse splitting. As this process continues, the peak intensity drops, stopping the collapse at $\tau = 0$. However, off-axis energy continues to focus at $\tau \neq 0$ such that two pulses are resolved.[8]

Numerical solutions of Eq. (1) have been performed, and a typical result is shown in Fig. 3. The initial field, $\tilde{\mathcal{E}}(r, z = 0, \tau)$, is taken to be a real hyperbolic secant in time and a real Gaussian in space. All parameters of the model are set equal to the experimental values given above, with the FWHM of the temporal and spatial profiles being 92 fs and 70 μm, respectively. In addition, a value of $k_0'' = 360$ fs^2/cm is used for the GVD in fused silica.[15] The peak power is 4.9 MW, in good agreement with the experimental conditions that led to clear pulse splitting [see Fig. 1(c)]. As Fig. 3 shows, the predicted output is symmetric, as expected from Eq. (1) when it is solved with symmetric initial conditions. The inset of Fig. 3 is the corresponding surface plot of the intensity, showing that the energy

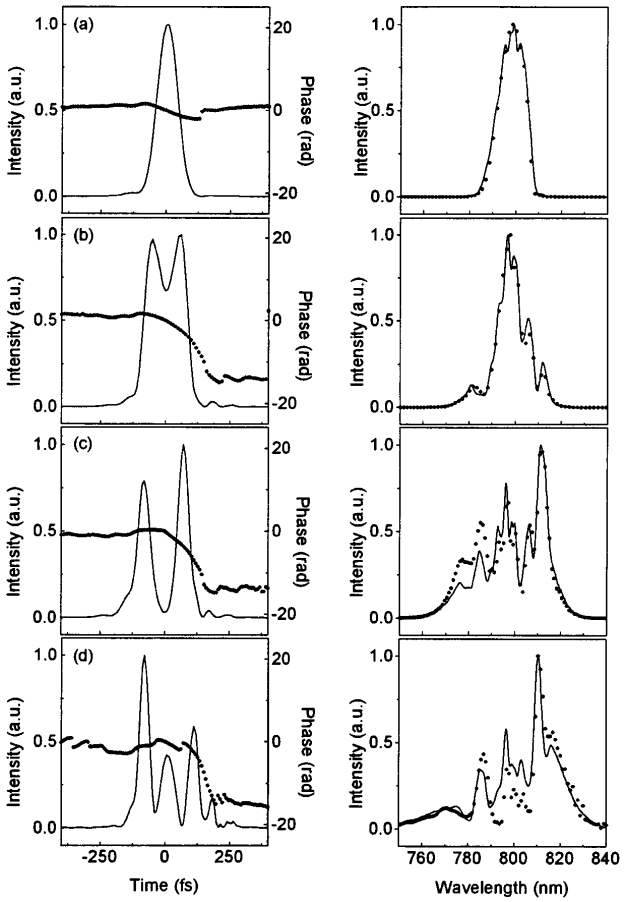

Fig. 1. Left, recovered electric-field intensity (thin solid curves, left axes) and phase (points, right axes). Right, corresponding measured (solid curves) and recovered (points) spectral intensities. The top row shows the input field, and the descending rows show the propagated fields for input peak powers of 4.5, 5.0, and 5.9 MW, successively.

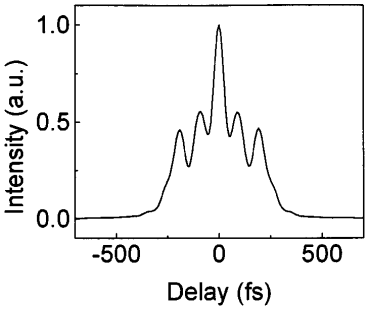

Fig. 2. Measured intensity autocorrelation for the field presented in Fig. 1(d).

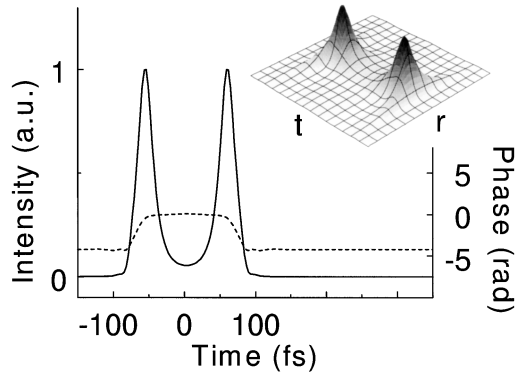

Fig. 3. Calculated on-axis intensity (solid curve) and phase (dashed curve) of split pulses. Inset, corresponding surface plot of the intensity as a function of both time (t) and radius (r).

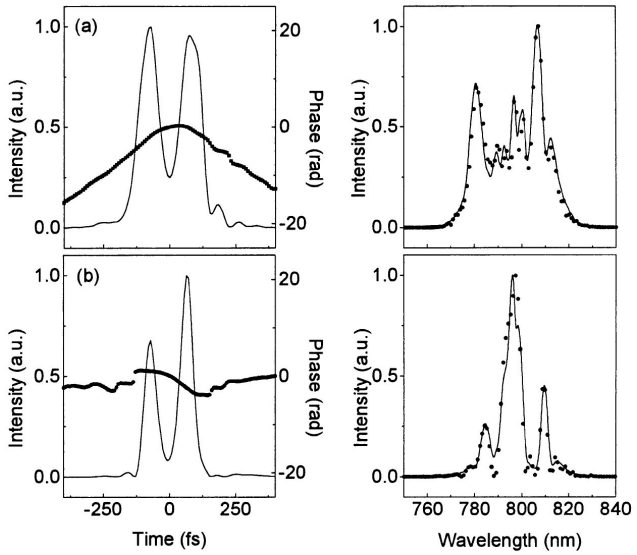

Fig. 4. Measured fields for (a) upchirped and (b) downchirped input. Left, recovered intensity (solid curves, left axes) and phase (points, right axes). Right, corresponding measured (solid curves) and recovered (points) spectral intensities.

remains well localized in space, although small oscillations do occur at larger radii. It is not yet clear what causes the temporal asymmetry in the corresponding experimental data. It could be the result of an asymmetric input, or it could be that Eq. (1) does not include phenomena such as third-order dispersion, self-steepening, and nonlocal mechanisms. We anticipate that further measurements and additions to the theory will provide understanding of which physical mechanisms are most important in this process.

The data of Fig. 4 illustrate that variations in the phase of the input can strongly affect the output. Here we present retrieved fields from the SHG FROG measurement after propagation of an input that is upchirped, Fig. 4(a), or downchirped, Fig. 4(b). We add the mostly linear chirp by varying the length of the compressor stage after the amplifier, and the time–bandwidth product of the input pulse in both cases is ~0.8. With the appropriate peak power, both situations result in pulse splitting; however, we see that for the upchirped input the split pulses are broader than for the downchirped input. In addition, the spectrum corresponding to the downchirped input has less modulation and is narrower than that of the upchirped input. On a basic level we can understand this situation by noting that both +GVD and SPM (with $+n_2$) act to produce positive, linear chirp over the central portion of the pulse. Thus the propagation-induced upchirp adds to the initial upchirp and results in broader pulses with enhanced oscillations on the spectrum. However, the downchirp on the input negates the propagation-induced upchirp, except in the pulse wings. The result is narrower pulses at the output (~2.5× less than input), with less spectral ringing.[9]

In conclusion, these measurements demonstrate the value of SHG FROG for the study of complex propagation problems. We have shown that pulse splitting in a nonlinear, dispersive medium leads to subpulses that are almost 2× shorter than the input and that the process is not generally symmetric. In addition, we present measurements to demonstrate the important role that the input phase can play. We anticipate that these and similar measurements will lead to a more comprehensive picture of nonlinear pulse propagation in the high-intensity regime and the theories used to describe it.

This research was supported by the National Science Foundation and the National Institute of Standards and Technology.

References

1. J.-C. Diels, J. J. Fontaine, I. C. McMichael, and F. Simoni, Appl. Opt. **24,** 1270 (1985).
2. Y. Ishida, K. Naganuma, and T. Yajima, IEEE J. Quantum Electron. **QE-21,** 69 (1985).
3. G. Taft, A. Rundquist, M. M. Murnane, H. C. Kapteyn, K. W. DeLong, R. Trebino, and I. P. Christov, Opt. Lett. **20,** 743 (1995).
4. E. T. J. Nibbering, M. A. Franco, B. S. Prade, G. Grillon, C. LeBlanc, and A. Mysyrowicz, Opt. Commun. **119,** 479 (1995); E. T. J. Nibbering, G. Grillon, M. A. Franco, B. S. Prade, and A. Mysyrowicz, J. Opt. Soc. Am. B **14,** 650 (1997).
5. A. J. Taylor, G. Rodriguez, and T. S. Clement, Opt. Lett. **21,** 1812 (1996).
6. J. M. Dudley, L. P. Barry, P. G. Bollond, J. D. Harvey, R. Leonhardt, and P. D. Drummond, Opt. Lett. **22,** 457 (1997).
7. P. Chernev and V. Petrov, Opt. Lett. **17,** 172 (1992).
8. J. E. Rothenberg, Opt. Lett. **17,** 583 (1992).
9. G. P. Agrawal, *Nonlinear Fiber Optics* (Academic, San Diego, Calif., 1989).
10. J. K. Ranka, R. W. Schirmer, and A. L. Gaeta, Phys. Rev. Lett. **77,** 3783 (1996).
11. R. Trebino, K. W. DeLong, D. N. Fittinghoff, J. N. Sweetser, M. A. Krumbügel, B. A. Richman, and D. J. Kane, Rev. Sci. Instrum. **68,** 3277 (1997).
12. G. Taft, A. Rundquist, M. M. Murnane, I. P. Christov, H. C. Kapteyn, K. W. DeLong, D. N. Fittinghoff, M. A. Krumbügel, J. N. Sweetser, and R. Trebino, IEEE J. Sel. Topics Quantum Electron. **2,** 575 (1996).
13. R. W. Boyd, *Nonlinear Optics* (Academic, San Diego, Calif., 1992).
14. J. H. Marburger and W. G. Wagner, IEEE J. Quantum Electron. **QE-3,** 415 (1967).
15. S. Diddams and J.-C. Diels, J. Opt. Soc. Am. B **13,** 1120 (1996).